



## Functionalizing Multifunctional Fe<sub>3</sub>O<sub>4</sub> Nanoparticle-Based Biocompatible, Magnetic and Photoluminescent Nanohybrids: Preparation and Characterization

DUY TRINH NGUYEN<sup>1,2</sup>, PHU THUONG NHAN NGUYEN<sup>1</sup>, THIEN HIEN TRAN<sup>1</sup>, DAI HAI NGUYEN<sup>3</sup>, DAI VIET N. VO<sup>4</sup>, MD. RAFIQUIL ISLAM<sup>5</sup>, KWON TAEK LIM<sup>5</sup>, SANG THANH VO<sup>1</sup> and LONG GIANG BACH<sup>1,2,\*</sup>

<sup>1</sup>NTT Hi-Tech Institute, Nguyen Tat Thanh University, Ho Chi Minh City, 700000, Vietnam

<sup>2</sup>Graduate University of Science and Technology, Vietnam Academy of Science and Technology, Ha Noi City, 100000, Vietnam

<sup>3</sup>Institute of Applied Materials Science, Vietnam Academy of Science and Technology, Ho Chi Minh City, 700000, Vietnam

<sup>4</sup>Faculty of Chemical and Natural Resources Engineering, Universiti Malaysia Pahang, 26300, Pahang, Malaysia

<sup>5</sup>Department of Display Engineering, Pukyong National University, Busan 608-737, Republic of Korea

\*Corresponding author: Fax: +84 2839404759; Tel: +84 969294297; E-mail: [blgiangntt@gmail.com](mailto:blgiangntt@gmail.com); [blgiang@ntt.edu.vn](mailto:blgiang@ntt.edu.vn)

Received: 28 July 2018;

Accepted: 9 October 2018;

Published online: 27 February 2019;

AJC-19283

A combination of ring-opening polymerization (ROP) and coordination chemistry methodology has been expanded for the synthesis of a multifunctional, biocompatible, magnetic, luminescent nanohybrid complex comprising magnetite (Fe<sub>3</sub>O<sub>4</sub>) nanoparticles (MNPs), poly( $\epsilon$ -caprolactone) (PCL) and europium ions (Eu<sup>3+</sup>). The structural and morphological characteristic of the nanohybrid intricate were studied by appropriate spectrum and physical researches. The superparamagnetic behaviour and unique Eu<sup>3+</sup> fluorescence properties with a high emission intensity of MNP-PCL-Eu<sup>3+</sup> were investigated *via* measurements with a superconducting quantum interference equipment magnetism and fluorescence spectroscopy.

**Keywords:** Fe<sub>3</sub>O<sub>4</sub> magnetic nanoparticles, Photoluminescent Eu<sup>3+</sup>, Ring-opening polymerization, Click coupling, Coordination chemistry.

### INTRODUCTION

Lately, because of desirable properties and relevant applications, nanocomposites have many functions, which have attracted the interest of the scientists. Due to potential bio-applications, which include magnetic targeted drug transport, magnetic resonance imaging disparity agents, hyperthermia treatment, biological separation, magnetite (Fe<sub>3</sub>O<sub>4</sub>) and nanoparticles (MNPs) are attracting considerable attention [1-5]. Nanoparticles (MNPs) can through quick biological decomposition when directly contacted to a biological scheme, because of anisotropic dipolar attraction. Hence, to pass these inconvenience and enable magnetite to be leveraged as biomedical intent, it need to pre-coated with materials that render it steady, biologically compatible and nontoxic in physiological media and can bind to intricas biological molecules [7-9]. Transplant polymers onto magnetic nanoparticles, then creating core-shell hybrid composites is the most usual and useful way to improve

the surface reformation. The polymer casing brings to springiness in controlling the component and configuration of the composites; so, in addition to the protective function of the magnetic nanoparticles opposed to combination of polymers casing, it also gives them with other role to increase the usefulness of their applications [6-12].

The method not only to maintain control of the polymer structure but also to achieving high coupling density is a potential method involved in applying modular in which nanoparticles carry a number that can control highly reactive surface species associated with unconnectedly arranged, finishing function polymers *via* an effective connection protocol. To date, the field of both materials science and polymers has remarkable attention to click chemistry. Because the module has the nature, high yield and selectivity of click reactions, it is attractive to conduct polymerization and modification of macromolecules [13-15]. Building blocks to be manufactured with apposite purposeful groups allowed by this method that

enable their connection in a single convergent stride. One thing to be attractive, the dendrimers, side-chain functional linear polymers, dendronized polymers and cross-linked materials was prepared by the copper(I)-catalyzed [3+2] Huisgen cycloaddition. A wide range of molecules on the surface of gold nanoparticles, silica nanoparticles and carbon nanotubes have demonstrated the use of click chemistry is common and highly selective, which is recognized as an ideal module method [16-19].

Over the past several decades, there has been a great deal of research focusing on polyester and co-polyesters have biological decomposition, which demonstrates the results of their ease of production and desired features. Some examples of degradable seams, controlled pharmaceutical transport matrices and temporary orthopedic fixtures are the proofs the physical properties and hydrolytic degradation shapes have made them pretty materials for use in various biomedical merchandises. Another example of this widely used in biomedical sciences is PCL, which is a hydrophobic and biodegradable polymer [20-23]. In addition, the biological decomposition property of aliphatic polyesters are produced by ROP of lactones, in which PCL being the main member of this family.

Multifunctional nanocomposites with both magnetic and fluorescent properties are expected to permit the engineering of unique nanoscale machine which has many functions that can be controlled using external magnetic areas. The lanthanide multiplexes displayed a high photoluminescence efficient with a long fluorescent lifetime, a narrow emission spectrum and large Stokes shifts when compared to normal luminescent materials. With these properties, organic dyes and radioactive probes have gradually been replaced by them and become a viable option. In particular, because of not toxic to people, lanthanides and their related coordination polymers are useful catalysts and against bacteria agents. Hybrid materials are available with luminescence properties, which have been fabricated by coordination or sol-gel chemistry reactions with lanthanide-doped inorganic and organic materials [24-30].

Because they represent combinations of the aforementioned aspects, hybrid systems based on isolated MNPs, including multi-composition hybrid have structures as nanometer and colloidal crystals with the size is nanometer as well as matrix-dispersed multiple materials and medium sized particles, will be highlighted. Herein, click reactions for preparing MNPs with biocompatible PCL with potential macromolecular ligands for  $\text{Eu}^{3+}$  coordination were explored. Multifunctional nanocomposites with both fluorescent and magnetic feature give a new exciting approach for many applications in biological field, including targeted drug delivery, bioimaging therapeutics and diagnostics.

## EXPERIMENTAL

Acetylene end-functionalized PCL with carboxyl end groups was prepared *via* ROP [25]. Magnetic nanoparticles were synthesized by the chemical coprecipitation of the  $\text{Fe}^{2+}$  and  $\text{Fe}^{3+}$  ions in alkaline media [28]. 3-Chloropropyltrimethoxysilane (CPTMS), NaOH, diethyl ether, sodium azide ( $\text{NaN}_3$ ), tetrahydrofuran (THF),  $\text{Eu}(\text{NO}_3)_3$ , CuBr, *N,N,N',N'',N'''*-pentamethyldiethylenetriamine (PMDETA), *N,N*-dimethylformamide (DMF), 1,10-phenanthroline (phen), anhydrous

methanol, toluene and aqueous  $\text{NH}_4\text{OH}$  were used as accepted. All aforementioned materials were bought from Sigma-Aldrich.

**Grafting of PCL onto MNPs *via* click chemistry:** The surface of MNPs was overlies with CPTMS *via* a reaction of silanization to achieve chloro-functionalized MNPs (MNP-Cl). Specifically, dehydrated toluene (40 mL) was mixed with 1 g of MNPs and 1.0 mL of CPTMS was added to the mixture, which was maintained at room temperature under the irradiation of ultrasonic waves for 30 min. The solution is stirred from a magnetic stirrer for a day at room temperature. Use a magnet to separate MNP-Cl, washed many times (over 3 times) with deionized water and dried under vacuum.

MNP-Cl was subsequently used to immobilize the azide group. In total, 500 mg of MNP-Cl was put in a 10 mL of aqueous solution and continue to add 0.1 g of  $\text{NaN}_3$ . The solution was left under a magnetic stirrer at room temperature for 2 day. After 2 days, the mixture was magnetically separated and use water to wash. Finally, dry overnight magnetite nanostructures (MNP-N<sub>3</sub>) at 40 °C in a clean vacuum oven.

Alkyne-f-PCL-COOH (55.8 mg), 2 mL of DMF and CuBr (3.9 mg) were put in a Schlenk tube 50 mL. In total, 10 mg of MNP-N<sub>3</sub> was dissolved in DMF at a volume of 3 mL and added to the tube. After that add 5.8 mL of PMDETA to the mixture. The system 3 freeze-pump-thaw cycles removed the gas of the tube, later placed in a thermostatic tank at 50 °C for 2 day. The solution was centrifuged at 0.5 h with 5000 rpm to finish the reaction; then remove the supernatant and use toluene washed the MNPs. After, the solution was centrifuged again with the same parameters as the first. This process was performed twice with toluene and once with  $\text{H}_2\text{O}$  to eliminate the polymer and copper catalyst no reaction. MNP-g-PCL-COOH was then dried in a clean vacuum oven overnight at 40 °C.

**Coordination reactions of  $\text{Eu}^{3+}$  with MNP-g-PCL-COOH:** Typically, 20 mg MNP-g-PCL-COOH was diffused in 5 mL ethanol 99.5 %. Later, the pH of the resultant solution was adjusted to 6-7 through 1,10-phenanthroline solution (0.9 mL) was added drop-wise and use NaOH aqueous solution. After, the mixed solution was slowly dropped a  $\text{Eu}(\text{NO}_3)_3$  was dispersed ethanol solution (0.9 mL) at maximum 10 min. Stir the reaction solution at room temperature for 5 h (followed by aging overnight) to obtain the product, then wash continuously with ethanol and vacuum drying for 2 days. The product was repeatedly washed with ethanol and dried below vacuum (at 40 °C) for 2 days.

**Characterization techniques:** We have studied the surface composition of samples through X-ray photoelectron spectroscopy (XPS; Thermo VG Multilab 2000) with  $\text{AlK}_{\alpha}$  radiation in an ultrahigh vacuum. Using PerkinElmer Pyris 1 (USA) analyzer to perform thermogravimetric analysis (TGA). The products were scanned in the temperature from 50 to 800 °C with a heating rate of 10 °C  $\text{min}^{-1}$  by a continuous nitrogen flow. We used an F-4500 spectrofluorometer (Hitachi, Japan) with a 352 nm excitation source to record the photoluminescence (PL) spectra. We used a superconducting quantum interference machine magnetometer (USA) to determine the magnetic properties. Field-emission scanning electron microscopy (FESEM) in conjunction with energy-dispersive

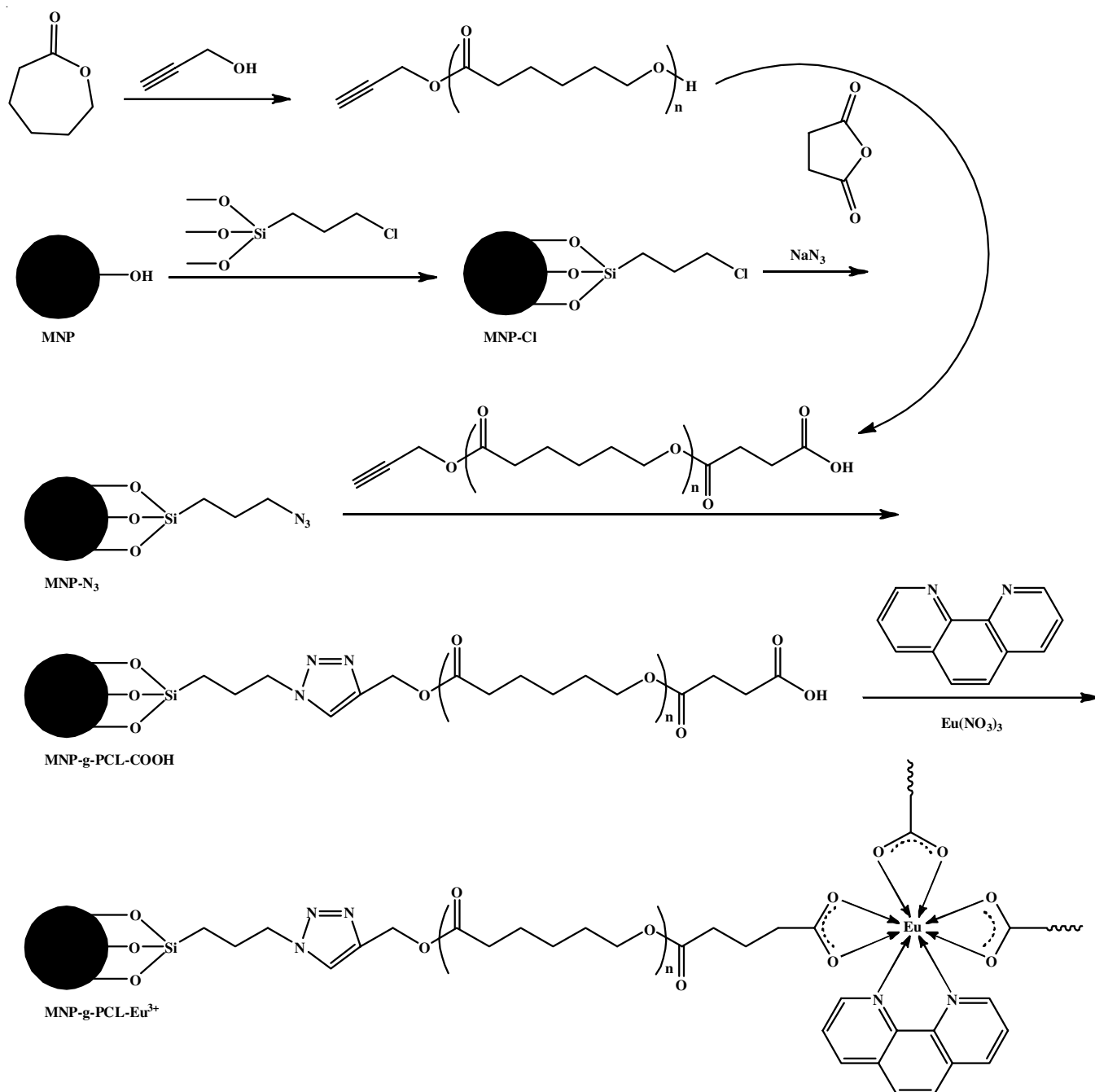
X-ray spectroscopy (EDX, Japan) was treated so that the nanohybrids could determine the elemental composition and morphology.

## RESULTS AND DISCUSSION

The overall strategy for preparing PCL-grafted MNPs was to use click chemistry with multicarboxyl groups on the exterior coatings. It involves coordination with trivalent europium ions (Eu<sup>3+</sup>) in presence of 1,10-phenanthroline (**Scheme-I**).

To confirm the MNP composition and evaluate the surface modification process, we investigated the functional surface of MNPs by conducting an X-ray photoelectron spectroscopy (Fig. 1). The MNPs' surface wide-scan spectrum was controlled by signals attributable to Fe, O and C. This result

indicate a characteristic doublet peak at about 711.0 eV, which corresponded to Fe2p (Fig. 1a). To have chloro-functionalized MNPs, CPTMS reacted with MNPs through a ligand-exchange reaction between triethoxysilane groups of CPTMS and hydroxyl groups on the surface of the MNPs. The wide-scan spectrum of MNP-Cl were clearly the typical signals for silicon (Si2p), chlorine (Cl2p), iron (Fe2p), oxygen (O1s) and carbon (C1s) with an intensity of 101.4, 199.7, 711.2, 530.4 and 285.0 eV, respectively. The silane-coupling procedure follows a condensation reaction to make an unchanging originator monolayer on the exterior of MNPs, as considered by the emergence of the Si and Cl signals in the XPS spectrum of MNP-Cl. The characteristic peaks assigned to Fe, SiO<sub>2</sub>, C, O and N appeared in the X-ray photoelectron spectra of MNP-N3, which indi-



**Scheme-I:** Reaction mechanism and coordination procedure of Eu<sup>3+</sup> coordination-functionalized magnetite (Fe<sub>3</sub>O<sub>4</sub>) nanoparticles (MNPs)-based complexes

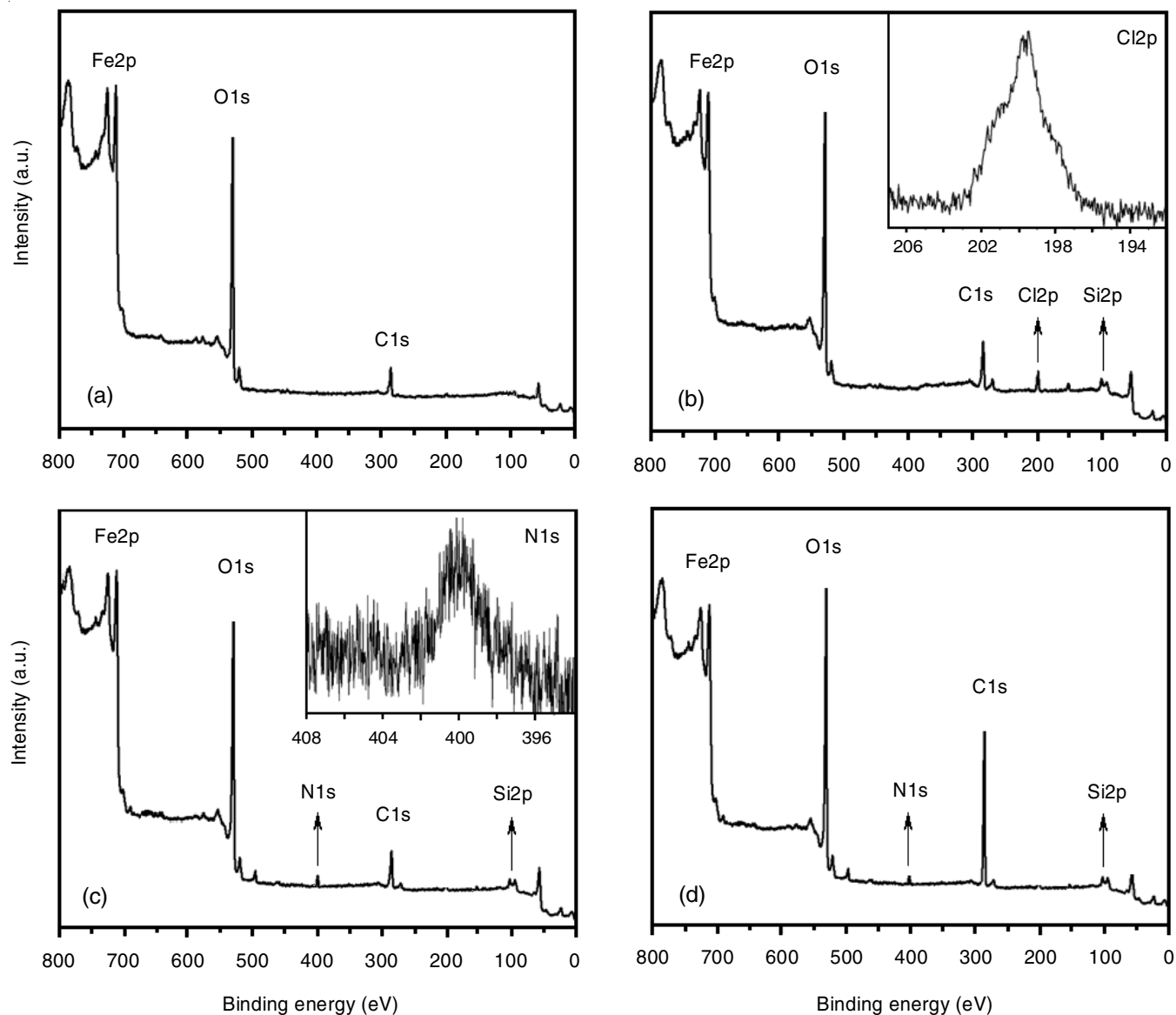


Fig. 1. X-ray photoelectron spectroscopy (XPS) survey scans of (a) MNPs, (b) MNP-Cl, (c) MNP-N<sub>3</sub> and (d) MNP-g-PCL-COOH

cated that the azido groups completely superseded the terminal chloro groups (Fig. 1e). In extension, at 399.7 eV indicated the characteristic signal for N1s. So, the XPS data showed that the azide groups modified the surface of MNPs. Fig. 1d presented the XPS wide-scan spectrum of MNP-g-PCL-COOH. The XPS scan of MNP-g-PCL-COOH indicated that a C1s peak with height a little altered to a higher binding energy, showing that the polymeric chains were straight attached from the surfaces of MNPs, after grafting PCL onto MNPs.

To consider the relative amount of biological compounds grafted onto MNPs, TGA measurements were performed. The results of which are shown in Fig. 2. TGA analyses of MNPs, MNP-Cl, MNP-N<sub>3</sub>, MNP-g-PCL-COOH and alkyne-PCL-COOH were conducted in the temperature range 50-800 °C. The total weight of MNPs lost about 4.1 % because of the removal of water absorbed (Fig. 2a). 10.2 % is the number of MPTMS grafted on the MNP after the reaction (Fig. 2b). MNP-N<sub>3</sub> exhibited a 2.39 % weight loss than MNP-Cl at 800 °C. The TGA curves for the PCL-coated MNPs are shown in

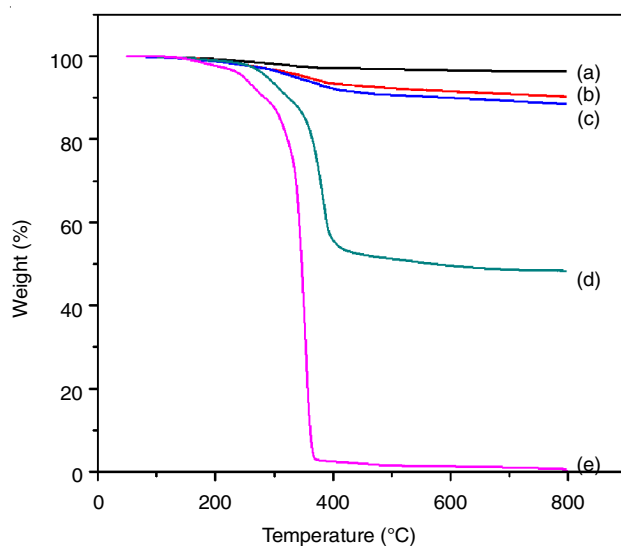


Fig. 2. Thermogravimetric analysis curves for (a) MNPs, (b) MNP-Cl, (c) MNP-N<sub>3</sub>, (d) MNP-g-PCL-COOH and (e) alkyne-f-PCL-COOH

Fig. 2d wherein they depict the transformation of the extant masses of the samples with heat. The main weight loss that happened at about 200 °C was ascribed to the decomposition of PCL. Thermogravimetric analysis also showed a magnetite content of about 40 %. We attributed that MNPs were created to enhance char formation in nanocomposites with higher temperature tolerance.

The MNPs attached to PCL to afford multicarboxyl-group external layers; the products were commonly used as templates or macromolecular ligands to combine 1,10-phenanthroline with Eu<sup>3+</sup>. To better understand the chemical composition of the prepared nanohybrid, we recorded the EDX spectra of MNPs and MNP-PCL-Eu nanohybrid samples, the results of which are shown in Fig. 3. The spectrum of MNPs intelligibly details the attendance of Fe along with C and O. In comparison with the spectrum of the MNP sample, the EDX spectrum of MNP-PCL-Eu showed the presence of Fe, SiO<sub>2</sub>, C, O, N and Eu. This consequence showed clearly indicated the successful coordination of Eu<sup>3+</sup> onto the surface of MNP-based hybrid complexes.

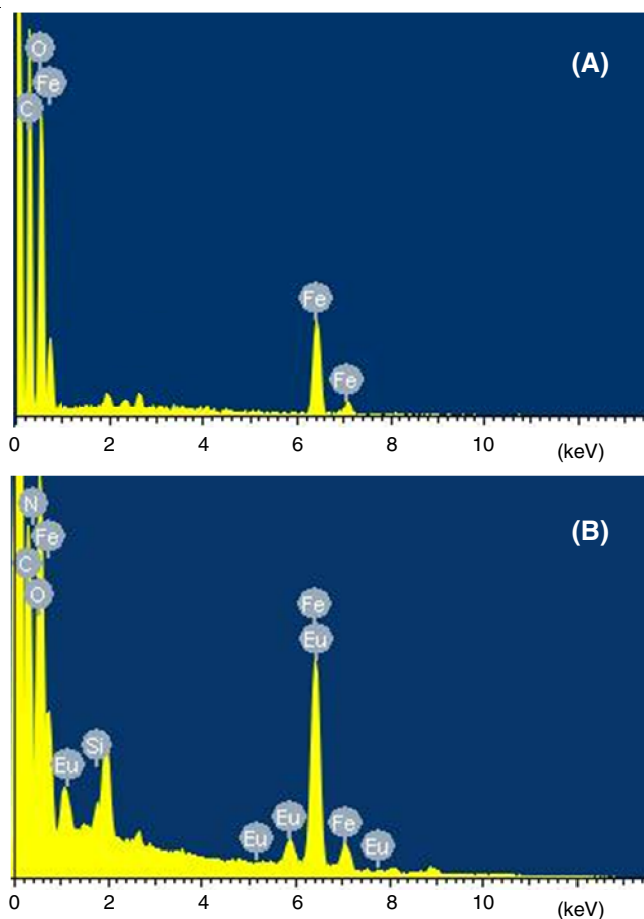


Fig. 3. Energy-dispersive X-ray spectroscopy (EDX) analysis of (A) MNPs and (B) MNP-PCL-Eu

The magnetic hysteresis loop of the magnetic MNP-g-PCL-Eu nanohybrids recorded at room temperature is shown in Fig. 4. The samples displayed superparamagnetic nature (*i.e.*, resonance and zero coercivity), which is critical for their application in biomedicine and biotechnology applications because it protects magnetic particle aggregation and permits

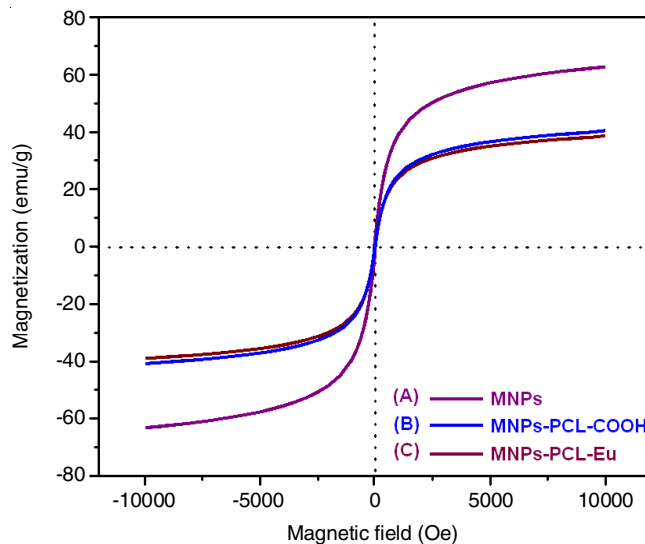


Fig. 4. Room-temperature hysteresis loops of the as-synthesized (A) MNPs, (B) MNP-PCL and (C) MNP-PCL-Eu

them to redisperse quickly when the magnetic field is removed. MNP, MNP-g-PCL-Eu and MNP-g-PCL-COOH are superparamagnetic according to field-dependent magnetic studies. Their saturated magnetization values are MNP: 62.3, MNP-g-PCL-Eu: 42.1 and MNP-g-PCL-COOH: 42.6 emu/g. In all cases, the hysteresis loops did not exhibit remanence and coercivity, ratifying that the coated nanoparticles of polymer exhibited superparamagnetic behaviour, which is appropriate for biomedical applications. The nanocomposites to be used in biomedical applications because they exhibit strong magnetization, allowing efficient magnetic delivery, concentration and separation through these magnetic properties.

The fluorescence spectra of the synthesized Eu<sup>3+</sup>-coordinated MNP-PCL nanohybrids are shown in Fig. 5. Under excitation at 260 nm, the conjugate displayed a series of bands at 578, 591, 610, 651 and 692 nm, which were respectively attributed to <sup>5</sup>D<sub>1</sub> → <sup>7</sup>F<sub>J</sub> (*J* = 0, 1, 2, 3 and 4) band transitions of Eu<sup>3+</sup>. In particular, because of the magnetic dipole transition

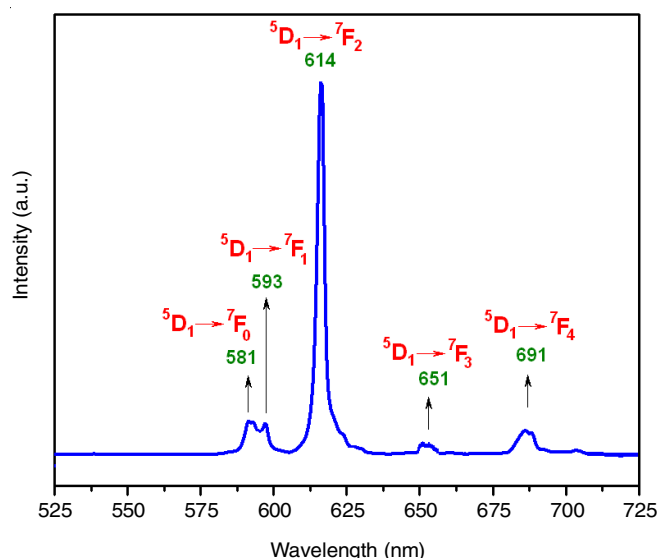


Fig. 5. Fluorescence spectra of Eu<sup>3+</sup> coordination MNP-PCL complexes with an excitation wavelength of 260 nm

and no response to the local structural environment led to the  ${}^5D_0 \rightarrow {}^7F_1$  transition. In contrast, because of electric dipole changes and response to the coordination environment of the  $\text{Eu}^{3+}$  ions so the red band may be due to  ${}^5D_0 \rightarrow {}^7F_2$  transition. The emission peak at 618 nm is higher than the 594 nm, which indicates that the  ${}^5D_0 \rightarrow {}^7F_2$  stream governs the  ${}^5D_0 \rightarrow {}^7F_1$  current and the low-symmetry in coordination environment of the  $\text{Eu}^{3+}$  centered ions. The reaction mechanism between the multicarboxyl groups in MNP-PCL and  $\text{Eu}^{3+}$  can be explained by the single electron couple on the oxygen atom of COO- of PCL-COOH is transferred to the blank electron orbit of the outer layer of  $\text{Eu}^{3+}$  ions and forms a united chelate circle.

## Conclusion

Herein, the synthesis of a new class of multifunction MNP-g-PCL- $\text{Eu}^{3+}$  nanohybrids is accomplished through coordination chemistry methodologies, click chemistry and the association of ROP. The results of XPS and EDX showed the presence of PCL on the MNPs' surface and photoluminescent  $\text{Eu}^{3+}$  coordination MNPs. The analysis of the magnetization curves showed that MNP-g-PCL- $\text{Eu}^{3+}$  exhibited superparamagnetic behaviour, which is critical for endovenous management in biomedical applications. In the MNP-g-PCL- $\text{Eu}^{3+}$  nanohybrid complex, a characteristic strong hypersensitive emission band of  $\text{Eu}^{3+}$  for ( ${}^5D_0 \rightarrow {}^7F_2$ ) transitions was observed at 614 nm. The reported work provides a general route for the synthesis of magnetic and luminescent multiple functional nanocomposites and this material gives up many applications in the general sciences, especially in biological systems.

## ACKNOWLEDGEMENTS

This work was supported by the Nguyen Tat Thanh University, VietNam and Pukyong National University, Republic of Korea.

## CONFLICT OF INTEREST

The authors declare that there is no conflict of interests regarding the publication of this article.

## REFERENCES

1. S. Behrens and I. Appel, *Curr. Opin. Biotechnol.*, **39**, 89 (2016); <https://doi.org/10.1016/j.copbio.2016.02.005>.
2. S. Bedanta, A. Barman, W. Kleemann, O. Petravic and T. Seki, *J. Nanomater.*, **2013**, Article ID 952540 (2013); <https://doi.org/10.1155/2013/952540>.
3. M.B. Gawande, Y. Monga, R. Zboril and R.K. Sharma, *Coord. Chem. Rev.*, **288**, 118 (2015); <https://doi.org/10.1016/j.ccr.2015.01.001>.
4. C. Huang, X. Qian and R. Yang, *Mater. Sci. Eng.: R: Reports*, **132**, 1 (2018); <https://doi.org/10.1016/j.mser.2018.06.002>.
5. D.W. Kim, L.G. Bach, S.S. Hong, C. Park and K.T. Lim, *Mol. Cryst. Liq. Cryst.*, **599**, 43, (2014); <https://doi.org/10.1080/15421406.2014.935919>.
6. L.G. Bach, M.R. Islam, J.T. Kim, S.Y. Seo and K.T. Lim, *Appl. Surf. Sci.*, **258**, 2959 (2012); <https://doi.org/10.1016/j.apsusc.2011.11.016>.
7. L.G. Bach, B.T.P. Quynh, M.R. Islam and K.T. Lim, *J. Nanosci. Nanotechnol.*, **16**, 12856 (2016); <https://doi.org/10.1166/jnn.2016.13651>.
8. R. Cha, J. Li, Y. Liu, Y. Zhang, Q. Xie and Mingming Zhang, *Colloids Surf. B: Biointerfaces*, **158**, 213 (2017); <https://doi.org/10.1016/j.colsurfb.2017.06.049>.
9. R. Hatel, M. Goumri, B. Ratier and M. Baitoul, *Mater. Chem. Phys.*, **193**, 156 (2017); <https://doi.org/10.1016/j.matchemphys.2017.02.013>.
10. K. Koc and E. Alveroglu, *J. Mol. Struct.*, **1089**, 66 (2015); <https://doi.org/10.1016/j.molstruc.2015.02.038>.
11. Y. Tang, H. Liu, J. Gao, X. Liu, X. Gao, X. Lu, G. Fang, J. Wang and J. Li, *Talanta*, **181**, 95 (2018); <https://doi.org/10.1016/j.talanta.2018.01.006>.
12. K.K. Jaiswal, D. Manikandan, R. Murugan and A.P. Ramaswamy, *Eur. Polym. J.*, **98**, 177 (2018); <https://doi.org/10.1016/j.eurpolymj.2017.11.005>.
13. L.G. Bach, X.T. Cao, M.R. Islam, Y.T. Jeong, J.S. Kim and K.T. Lim, *J. Nanosci. Nanotechnol.*, **16**, 2975 (2016); <https://doi.org/10.1166/jnn.2016.11049>.
14. Y. Li, X.H. Dong, Y. Zou, Z. Wang, K. Yue, M. Huang, H. Liu, X. Feng, Z. Lin, W. Zhang, W.B. Zhang and S.Z.D. Cheng, *Polymer*, **125**, 303 (2017); <https://doi.org/10.1016/j.polymer.2017.08.008>.
15. A. Lungu, J. Ghitman, A.I. Cernescu, A. Serafim, N.M. Florea, E. Vasile, and H. Iovu, *Polymer*, **145**, 324 (2018); <https://doi.org/10.1016/j.polymer.2018.05.015>.
16. J.C. Chen, W.Q. Luo, H.D. Wang, J. M. Xiang, H.F. Jin, F. Chen and Z.W. Cai, *Appl. Surf. Sci.*, **256**, 2490 (2010); <https://doi.org/10.1016/j.apsusc.2009.10.093>.
17. W. Limapichat and A. Basu, *J. Colloid Interface Sci.*, **318**, 140 (2008); <https://doi.org/10.1016/j.jcis.2007.09.054>.
18. M.V. Bermeshev and P.P. Chapala, *Progr. Polym. Sci.*, **84**, 1 (2018); <https://doi.org/10.1016/j.progpolymsci.2018.06.003>.
19. Y. Zou, L. Zhang, L. Yang, F. Zhu, M. Ding, F. Lin, Z. Wang and Y. Li, *J. Control. Rel.*, **273**, 160 (2018); <https://doi.org/10.1016/j.jconrel.2018.01.023>.
20. P. Grossen, D. Witzigmann, S. Sieber and J. Huwyler, *J. Control. Rel.*, **260**, 46 (2017); <https://doi.org/10.1016/j.jconrel.2017.05.028>.
21. X. Qi, Y. Ren and X. Wang, *Int. Biodeterior. Biodegrad.*, **117**, 215 (2017); <https://doi.org/10.1016/j.ibiod.2017.01.010>.
22. F. Pahlevanzadeh, H.R. Bakhsheshi-Rad and E. Hamzah, *J. Mechan. Behav. Biomed. Mater.*, **82**, 257 (2018); <https://doi.org/10.1016/j.jmbbm.2018.03.016>.
23. J. Liu, D.Y. Lin, B. Wei and D.C. Martin, *Polymer*, **118**, 143 (2017); <https://doi.org/10.1016/j.polymer.2017.04.070>.
24. L. Sun, R. Wei, J. Feng and H. Zhang, *Coord. Chem. Rev.*, **364**, 10 (2018); <https://doi.org/10.1016/j.ccr.2018.03.007>.
25. L.G. Bach, B.T.P. Quynh, N.T. Thuong and V.T.T. Ho, *Mol. Cryst. Liq. Cryst.*, **644**, 175 (2017); <https://doi.org/10.1080/15421406.2016.1277476>.
26. J. Wang, S. Chen, H. Liu and W. Li, *J. Rare Earths*, **36**, 733 (2018); <https://doi.org/10.1016/j.jre.2018.01.006>.
27. L.G. Bach, X.T. Cao, M.R. Islam, H.G. Kim and K.T. Lim, *J. Nanosci. Nanotechnol.*, **15**, 5897 (2015); <https://doi.org/10.1166/jnn.2015.10438>.
28. S. Wang and L. Wang, *TrAC Trends Anal. Chem.*, **62**, 123 (2014); <https://doi.org/10.1016/j.trac.2014.07.011>.
29. L.G. Bach, Q.T.P. Bui, X.T. Cao, V.T.T. Ho and K.T. Lim, *Polym. Bull.*, **73**, 2627 (2016); <https://doi.org/10.1007/s00289-016-1712-5>.
30. L.G. Bach, M.R. Islam, X.T. Cao, J.M. Park and K.T. Lim, *J. Alloys Compd.*, **582**, 22 (2014); <https://doi.org/10.1016/j.jallcom.2013.07.186>.